Size distribution for potentially unstable rock masses and in-situ rock blocks using LIDAR generated Digital Elevation Models

O. Mavrouli[1,3], J. Corominas[1], M. Jaboyedoff[2]

[1]Department of Geotechnical Engineering and Geosciences, Technical University of Catalonia, 08034, Barcelona, Spain

[2]Centre de recherche sur l'environnement terrestre Faculté des géosciences et de l'environnement, University of Lausanne, CH-1015 Lausanne, Switzerland

[3]International Centre for Numerical Methods in Engineering, CIMNE, 08034, Barcelona, Spain

Corresponding author: Olga Mavrouli, olga-christina.mavrouli@upc.edu, +34934010731

Keywords: rockfalls, hazard, magnitude, frequency, Lidar, Terrestrial Laser Scanner

Abstract

In this paper, two analytical procedures which are independent from the existence of empirical data are presented for the calculation of (i) the size distribution of potentially unstable rock masses that expresses the potential rockfall size distribution, PRSD, including big volumes corresponding to potential rare events with low susceptibility of failure and (ii) the in-situ block distribution on the slope face, IBSD. Two approaches are respectively used. The first one involves the detection of kinematically unstable surfaces on a DEM and on orthophotos and the calculation of the volumes resting on them. For the second one the in-situ block volumes formed by the intersection of the existing discontinuity sets are calculated using a high-resolution DEM. The procedures are presented through an application example at the country of Andorra and in particular at the chute of Forat Negre. The results from the first procedure indicate that it is kinematically possible to have mobilised volumes of some thousands of cubic meters, however these are considered rare events with low susceptibility of failure. The size distribution of potentially unstable rock masses for big volume events was well fitted by a power-law with an exponent of -0.5. The in-situ block distribution on the slope face from the second procedure, assuming three types of intersection between the joints of the existing discontinuity sets and two extreme cases of discontinuity persistence, was also found

to follow a power-law, but with an exponent of -1.3. The comparison with the observed in the field block volume distribution on the slope face indicates that in reality discontinuities have a very high persistence and that considering only their visible trace length overestimates volumes, which is conservative.

1. Introduction

Rockfalls start with the detachment of rock from a steep slope along a surface on which small or no shear displacement takes place (Varnes, 1978). This definition involves very different situations. Some basic classifications have been given by Cruden and Varnes (1996) and Hungr et al. (2014), who differentiate simple falls from the detachment of large rock masses such as sturzstroms (Hsu and Kenneth, 1975), also called rockfall avalanches (Varnes, 1958) or rock avalanches (Evans et al., 1989). The former usually refer to fragmental rockfalls i.e. rockfall characterised by one or several independently moving fragments, while the second ones to extremely rapid mass flows of dry debris created by large falls and slides. The work presented here refers to fragmental rockfalls smaller than 10^5 m^3, although the volume limit is not still well-defined in the global literature (Evans and Hungr, 1993). For fragmental rockfalls the size and velocity of the individual blocks determine the intensity of an event.

The quantification of the rockfall hazard requires information on the expected probability or temporal frequency of rockfalls of a given magnitude (size), usually in the form of magnitude-frequency relations. The rockfall magnitude-frequency relation is governed by many parameters. The most important are the number, dip direction and dip of the existing discontinuities and their mechanical properties, the local topographical conditions, the rock mass strength, as well as the intensity of the triggering factors (earthquake, rainfall…) and whether they are sufficient to mobilise masses of a given magnitude. When the inventory time-frame is short, information is often missing with reference to the potential for large volume events, corresponding to rare events. However, in reality, even if large failures have not occurred in the inventoried past, the possibility for future ones still exists. To check the potential for big events several researchers suggest the use of the same power-law as for smaller events (Hungr et al. 1999, Dussauge et al. 2002, Guzzetti et al. 2003). However as Rohmer and Dewez (2012) outlined, the vision of very large extreme event (catastrophic) frequency being an extrapolation of the power laws fitted on small and intermediate events has been challenged in various contexts (Dorren et al. 2011, Dussauge et al., 2002). Sornette (2002) proposed viewing such catastrophic events as “outliers” from the power-law model, i.e. they deviate by an abnormal large distance from the extrapolated prediction. Thus there is the need for alternative methodologies for the detection of potential large instabilities.

Moreover the fragmentation effect on the initial mass and the size and velocity of the fragments are also very important for the rockfall hazard and risk assessment (Jaboyedoff et al. 2005 and Corominas et al. 2012). Although fragmentation is recognised as a complex process (Chau et al. 2002; Zhang et al. 2000),

Wang and Tonon (2010) and Locat et al. (2006) have identified the effect of some important parameters as the presence of discontinuities and their persistence in the detached rock mass.

Thus a common key-point for obtaining both of the afore-mentioned pieces of information is the characteristics of the discontinuity sets that are present in the slope face. Their role is double. They delimit the potentially mobilised volumes, thus affecting the rockfall size-distribution. Additionally, they represent weak planes inside the detached rockfall masses along which those break apart upon impact on the ground surface. Although some discontinuities might not break, the delimitation of the rock blocks of a certain volume by them is related to the fragmentation effect.

a) Volume of potentially unstable rock masses

A way towards the construction of a rockfall frequency-magnitude relation is the determination of the potentially mobilised volumes on the rock wall from the discontinuity network. These are the volumes that under given conditions may detach and produce rockfalls events. From now on, the distribution of these volumes will be referred to as potential rockfall size distribution (PRSD). As the distribution of the rockfall scars on the cliff face is an indicator of the rockfall activity over the last hundreds or thousands of years (Santana et al. 2012), the distribution of the potentially unstable rockfall masses on the cliff face as well. The objective of this work was the development of a procedure to calculate it. Focus is given on the possibility of having large rock masses mobilised, leading to events bigger than the observed ones so far, to calculate their volume and to provide an indication of their relative frequency in the rock mass. The PRSD is based on the detection and measurement of the size of potentially kinematically unstable rock masses on a digital elevation model of a steep slope face, where unfavourably dipping discontinuity sets are present.

b) Size distribution of the in-situ rock blocks

To get a clue on the size of the fallen blocks (or rock fragments) generated by a rockfall event after a potential fragmentation, the distribution of the individual rock volumes within the detachable rock mass on the face of the slope was investigated. The individual volumes are formed by the intersection of the existing discontinuity sets (Lu and Latham, 1999; Nocilla et al. 2009; Elmouttie and Poropat 2011). This distribution is herein called in-situ block size distribution (IBSD). In rock blasting research a correlation is often indicated between the size distribution of the in-situ blocks on a rocky wall and the resultant fragments after blasting (Aler et al., 1996; Lizotte and Scolbe, 1994). This is physically interpreted by the fact that both depend strongly on the initial structure of the rock mass and the discontinuities network. Additionally several researchers have developed sophisticated models for the calculation of the IBSD based on the discontinuity network as those described by Wang and Tonon (2010) and Elmouttie and Poropat (2011). Here a simple procedure was developed, which uses discontinuity data obtained by a point cloud.

In a few words, the main objective of this work was the development of two simple procedures for the calculation of the PRSD and IBSD on the slope face right on the source, based on the existing discontinuity sets and their spacing. The two procedures presented here for the evaluation of the PRSD and IBSD are independent one from each other and the provided information is not interrelated but complementary. This work forms part of an on-going investigation for the correlation of the PRSD with the rockfall frequency-magnitude and of the IBSD with the fallen blocks size distribution so that they can be introduced directly into the hazard assessment; however this is out of the scope of this paper.

2. Proposed methodology based on Terrestrial Laser Scanning data

2.1 Use of Terrestrial Laser Scanning data for rockfall investigation

Field investigation may have several restrictions related to access limitations, security issues and time-consuming and labour-intensive work requirements. Due to these reasons, the massive investigation of an entire slope for its structural characterization is almost impossible, especially if intensely fractured. To overcome these limitations, we propose the use of digital elevation models DEM, obtained with Terrestrial Laser Scanner data.

In the last decades, important advances have been achieved in remote-sensing techniques such as Terrestrial Laser Scanners TLS or LIDAR (LIght Detection and Ranging) for the capturing of point clouds representing three dimensional surfaces. TLS present the advantage of obtaining data of high precision and accuracy, easily, quickly and without access restrictions and in a digital format which offers flexibility for their massive elaboration (Slob et al., 2005; Slob and Hack, 2004). However several limitations exist as well, as for example in the case of scans that intrinsically suffer from "shadows" of missing data cast on surfaces by occluding objects (Sturznegger and Stead, 2009; Becker et al., 2009; Lato et al., 2009).

The advances in techniques for capturing point clouds have been followed by the development of methodologies that exploit these high resolution data, for applications related to the evaluation of rockfall susceptibility and hazard, starting from the reconstruction of surfaces for the creation of DEM (Hack, 1998; Kemeny and Post, 2003; Kemeny et al., 2006). These applications are explicitly described at Kemeny and Turner (2008) and Jaboyedoff et al. (2012). Amongst them are: the identification and characterization of discontinuity sets (Sturzenegger and Stead, 2009; Slob et al., 2005; Kemeny et al., 2006; Jaboyedoff et al., 2009; Gaich et al., 2006; Coggan et al., 2007; Birch, 2006; Poropat, 2006; Lato et al., 2009; Jaboyedoff et al., 2004, 2007, 2009; Derron et al., 2005), the detection of rockfall scars (Guerin et al. 2014; Oppikofer 2009; Santana et al. 2012), and the definition of potentially movable rock masses (Lato et al., 2009).

2.2 Description of the proposed methodology

The work presented in this paper includes mainly the two following procedures for:

(1) The calculation of the PRSD, from small to big rock mass volumes showing high to low susceptibility to failure respectively. This is achieved by the detection of kinematically unstable surfaces on a DEM and on orthophotos, and calculation of the rock mass volumes resting on them.

(2) The assessment of the IBSD on the slope face, by calculation of the volume of the prisms which are formed by the intersection of the existing discontinuity sets, based on data obtained by analysis of a DEM.

The necessary data for the application of the proposed procedure are a DEM and orthophotos of the study site. Especially for the second procedure a high resolution DEM is needed as for example those acquired by TLS point clouds.

Both procedures need as a prerequisite the identification of the main discontinuity sets. This is also made using the TLS point cloud and the COLTOP3D technique (Jaboyedoff et al., 2004, 2007, 2009; Derron et al., 2005). COLTOP3D is a tool allowing the elaboration of large point clouds and large regular grids of DEM. It permits to visualize the orientation of each discontinuity set by a unique colour, according to the dip direction and the dip of each point of the point cloud, after automatic attribution of a normal vector to it (Metzger et al., 2009). This facilitates the visual identification of discontinuity sets. Additionally, their properties may be evaluated by selecting a representative sample of points from the point cloud that correspond to each set and, then, by assessing statistically their average dip and dip direction.

Having identified the principal discontinuity sets for the study site, the determination of the potential failure mechanisms and of the discontinuity set(s) that contribute to the rockfall detachment is feasible. This is realised through kinematic analysis tests, which should be adjusted to the potential failure mechanisms (i.e. plane or wedge failure or toppling), according to the discontinuity network at each study site. For each specific failure mechanism, the respective conditions according to Markland (1972) and Hoek and Bray (1981) will define which discontinuities are unfavourable, depending on their average dip direction and dip with respect to the slope orientation and angle.

2.3 Calculation of the PRSD

The application of the first procedure involves the detection of the Potential Rockfall Size Distribution PRSD on the DEM. The unstable volumes are defined as those rock masses resting on joints that do not meet the stability criteria (Jaboyedoff et al., 2009; Derron et al., 2005). The method consists in the following steps:

Step 1: Using a DEM in raster format, we check compliance with the kinematic criteria for the stability of slopes described at Markland (1972) and Hoek and Bray (1981) at every cell of the raster to define whether

a given discontinuity is unfavourable or not. A discontinuity is unfavourable when (a) the joint dip direction and the slope orientation differ less than 20 degrees; (b) the joint dip angle is bigger than the friction angle and (c) the joint dip angle is smaller than the slope face angle. For step (b), the friction angle value depends on the rock joint characteristics and the infill material if any. For unfilled joints in granitic rock and volumes without any sign of displacement Gates et al. (2005) used the peak friction angle of the joints. Instead Di Luzio et al. (2013) adopted the residual friction angle in the case of a generic weathered joint surface filled with soft material. Further indications on the calculation of the shear strength of the rock joints involving the friction angle are given by Barton (2013) and Grasselli (2001).

Figure 1(i) describes the application of the kinematic criteria for a given slope, in every cell of the DEM raster. It is assumed that all joints are present in every cell. When two potentially unstable cells are contiguous, it is assumed that they form part of the same removable rock mass (Figure 1(ii)). The detected potentially unstable surfaces are overlaid on orthophotos for their visual validation. Additionally, the observation of the orthophotos facilitates the detection of smaller surfaces, if any, inside the previous ones, which stick out from the topographical relief and correspond to smaller potentially unstable surfaces.

Having identified the potential unstable cells and surfaces, the volumes of the corresponding removable rock masses should be obtained. To assess the total volume of the removable rock mass firstly the area of the unstable slope face, A, is calculated from the area of unstable cell(s), A_{cells} (Equation 1). A_{cells} is obtained using ArcGis utilities.

$$A = \frac{A_{cells}}{\cos\alpha} \quad (1)$$

Where:

A: area of the removable rock mass

A_{cells}: area of the unstable(s) cell(s)

α: slope dip angle (average value over the area A)

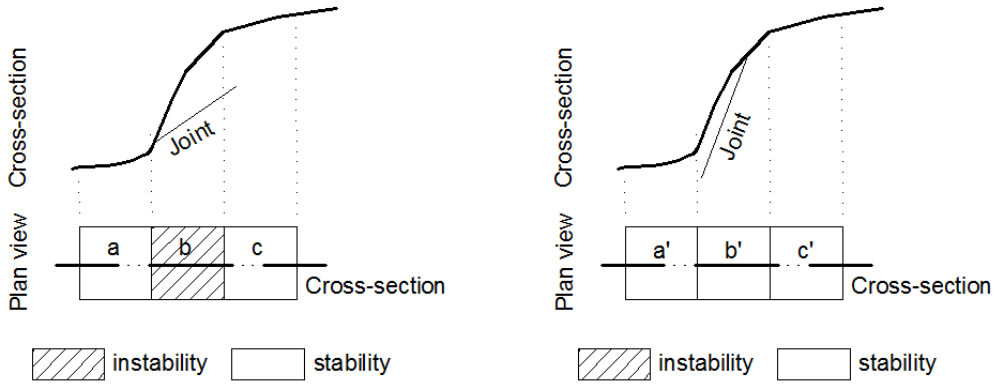

CASE I - pixel "b" is unstable according to the Markland kinematical test
- dip direction joint- dip direction slope < 20° and
- joint dip angle < slope face angle

CASE II - pixel "b"" is stable according to the Markland kinematical test
- dip direction joint-dip direction slope > 20° or
- joint dip angle > slope face angle

Fig. 1(i) Application of the kinematic criteria to a given slope (cross section), in every cell of the DEM raster (plan view) on the condition that the joint dip angle is greater than the friction angle.

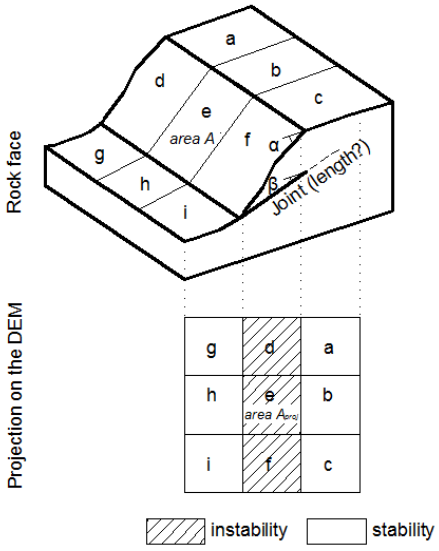

Fig. 1(ii) The rock face and its projection on the DEM raster. Unions of contiguous cells are assumed to indicate continuous removable rock masses.

Step 2: Besides the area of the slope face, the length of the unfavourable joint is required for the calculation of the removable rock mass (Figure 1(ii)). In most cases, this information is not available. If the

persistence of the unstable joints is to be considered infinite, this would describe an extremely conservative scenario and in most cases not realistic. In the same figure, that would be the case of considering unstable all three cells "a, b, and c".

For intensely fractured rock masses, the unfavourable discontinuities are usually intersected by others at relatively short distances from the slope face, defining smaller potentially unstable rock masses. Thus, a relation between the volume and the joint length was established, which is based on two alternative considerations: either equivalent cubic volumes are assumed, with all edges equal, or prismatic volumes where the persistence's length is half of the height in the previous case. Scar volumes were assumed to be prismatic. Palmstrom (2005) indicated that for angles of 60° or more between the prism base and height, the inaccuracy imposed by a simplified measurement that considers all angles of the prism 90° is limited. This is also valid for the study area as explained in Section 3.

According to Hantz (2011), in a general formulation, the relationship between the volume V and the length L of the fallen compartments depends on the internal structure of the rock wall and it may be written:

$$V = kL^3 \quad (2)$$

where

k: shape coefficient (1 for unknown volumes)

Assuming an equivalent cubic shape, the equivalent edge is equal to $L= A^{0.5}$ and the falling compartments, corresponding here to potentially unstable rockfall masses, can be calculated by:

$$V \simeq A^{3/2} \quad (3)$$

Where

V: the volume of the potentially removable rock mass

A: the area of the potentially removable rock mass

Accordingly for equivalent prismatic volumes with length L of the joint equal to half of the height of the afore-mentioned cubic volumes, the volumes can be calculated as:

$$V \simeq 0.5\, A^{3/2} \quad (4)$$

The afore-mentioned assumptions describe very conservative scenarios which yield very big volumes. The presence and intersection of persistent joints that kinematically permit the detachment of rock masses from the slope face in every cell of the DEM in reality has a very low probability. This is why these volumes correspond to rare events with low susceptibility of failure.

The proposed methodology takes into consideration rockfalls resulting from stepped-path failures. Stepped-path failures are represented on the DEM when adjacent cells are affected by joints of the same set but that are situated at different levels instead of a single one.

Furthermore it applies to rock mass volumes containing several discontinuity sets. For slopes with one predominant and continuous discontinuity set and with scarcity of discontinuities intersecting it, large volumes of greater depth/surface ratio than the equivalent cubic or prismatic volumes that are assumed here can be formed, even for small slope faces, as for example the typical translational landslides developing on stratification surfaces (Cruden and Hungr, 1986).

2.4 Calculation of the IBSD

For the second procedure, the point cloud DEM obtained by TLS is used to calculate the In situ Block Size Distribution IBSD. We make the basic assumption that the in-situ blocks are formed by the intersection of the discontinuities which are present at the slope and their volume depends on the spacing of the latter, or in other terms, on the distance between two successive discontinuities of the same set. The intersection of the discontinuities has to be investigated in order to determine the shape of the in-situ volumes. This can be realized by direct field observations on the study site in combination with visual inspection of the point cloud on COLTOP3D.

The rock blocks are assumed to be bounded by the existing discontinuities as they intersect each other. These intersections leading to the formation of rock blocks have to be identified. All sets that produce such intersections are taken into consideration, irrespectively of whether the blocks are kinematically unfavourable as in the previous step.

For every discontinuity set that contributes to the formation of volumes, the points belonging to it are isolated from the rest of the point cloud. The points which on visual criterion are detected to belong to the same surface of the slope are grouped and a plane is automatically fitted to them using the software Polyworks. This is repeated separately for all the surfaces within each set. During the fitting of planes, neighbouring points that exceed a maximum in-between distance and angular deviation are filtered out. The calibration of the used thresholds is made by observations of the photos of the area, so as to get realistic planes fitted.

Then to assess the average spacing for each discontinuity set, Polyworks utilities were used to measure manually, one by one for all planes, the perpendicular distance from an origin point on a plane near its centre, to its neighbouring plane, at a representative sample of the cliff. Two extreme assumptions are made for the calculation of the average spacing: a) discontinuity sets are of infinite persistence, thus having the minimum value of spacing between them, which is a theoretical case, or b) discontinuity sets are of finite persistence having an average spacing equal to the average perpendicular distance between the quasi-parallel surfaces measured on the DEM and considering only the visible trace length. The average spacing at a representative area of the cliff for the two assumptions on the discontinuity persistence is calculated according to Jaboyedoff (1996 and 2001) from the traces of the joints for every discontinuity set, as shown

in Figure 2. The software Mattercliff (Délèze et al., 2003) was used. For the assumption (a) the average spacing is the smallest because the joints are of infinite persistence so inside the sampling window the number of intersections with a scanline is the greatest (Figure 2). For the same sampling window and for the assumption (b) only the visible trace length of the discontinuities at each plane is considered and the number of intersections with a scanline is smaller.

The distribution of spacing massively over the slope cliff can be given by a negative exponential distribution as suggested by various researchers (Krishna et al., 2009; Priest and Hudson, 1981; Wallis and King, 1981; and Kulatilake et al., 1995), with the following probability density function:

$$P(x) = \frac{1}{\bar{s}} e^{-\frac{x}{\bar{s}}}, \quad x \geq 0 \tag{5}$$

$\bar{s}$: mean discontinuity spacing

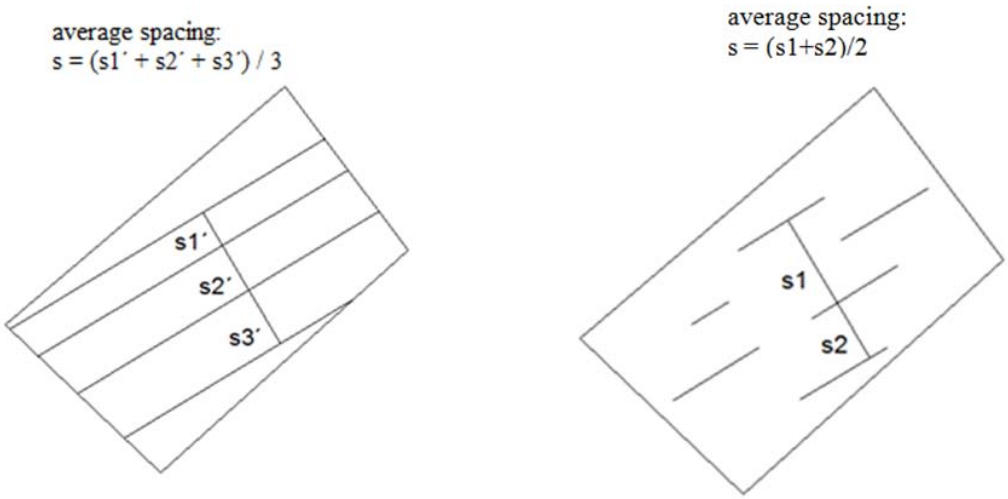

Fig. 2 Indicative calculation of the average spacing considering discontinuities of infinite (case a – left) and discontinuities of finite persistence (case b – right)

IBSD can then be assessed in function of the discontinuity spacings for the selected intersecting sets. For quasi-regular parallelepipeds with edges equal to the average spacing and infinite discontinuities, a regular parallelepiped can be considered for the shape of the blocks. For finite discontinuities, an equivalent quasi-regular parallelepiped can be also considered, with edges equal to the respective average spacing. So, these volumes can be approximated by equivalent prismatic volumes by (Kim et al., 2007):

$$Vo = s_{j1} * s_{j2} * s_{j3} \quad (6)$$

s_{j1}, s_{j2}, s_{j3}: discontinuity spacing of the bounding intersecting discontinuity sets

The volume variation due to the variation of spacings over the slope is probabilistically accounted for, with a Monte Carlo simulation where spacings follow the negative exponential distribution. These results yield a probabilistic relation for the IBSD for every intersection of discontinuities and infinite or finite persistence assumptions.

3 Application

The proposed procedures are presented through an application example at a selected study-site. It is the slope situated above the urban area of Santa Coloma, in the country of Andorra, in the Middle Eastern Pyrenees.

3.1 Description of the study-area

For the wider area, the retreat of the Pleistocene glaciers about 20000 years ago has resulted in a typical U-shape valley profile. The subsequent occurrence of morphogenetic processes such as decompression and freeze-thaw cycles has resulted in intense rockfall activity under non-seismic conditions. The slope next to the valley exceeds the 1000 m and the rock material is basically intensely fractured granodiorite. Its special interest is ought to the rockfall risk for the buildings which lie at the low part of the slope.

In particular we investigate the chute of Forat Negre (Figure 3) where unstable volumes are present at the left and right side of the chute. During the last decades various rockfall events of magnitude up to some hundreds of cubic meters occurred and produced blocks up to 30 m^3 reaching and damaging buildings and injuring people.

The wider area is characterized by intense rockfall activity, of approximate annual frequency 0.5 events/year (Moya et al. 2010), with rockfall volumes, varying from a few cubic to several thousand meters. An inventory of rockfall events for the area was compiled by Copons (2004), including events since the end of the 1960s. For that period and, strictly, for the investigated slope, the rockfall magnitudes are limited up to some hundreds of cubic meters. As for example the event of April 2004 of a rockfall of 25 m^3 resulted in fragments up to 4 m^3. On April 2008, a rock mass volume of approximately 150 m^3 was detached from the slope face with the biggest fallen block approximately of 30 m^3. The latest event was registered on February 2014, when a mass of approximately 20 m^3 produced various blocks of maximum size 4.5 m^3, and a block of 3.50 m^3 reached the urban area and penetrated the wall of a workshop.

Nevertheless, higher rockfall magnitudes of the order of 1000 m^3 have been observed at adjacent chutes (at the Tartera de la Pica on April 1969), implying a potential for higher volumes also for the study-site. Nowadays, high-energy dissipative steel fences are installed at the bottom of the slope, which at recent rockfalls were proved very efficient at retaining the majority of blocks. However, failure at impeding the blocks reaching the buildings has also been observed which was caused by the excessive rotation of the vertical supports of the nets, thus permitting the blocks to fly over them. Consequently their efficiency cannot be guaranteed for high magnitude events leading to considerable rotations of the supports and so the occurrence of the latter should be studied. To this purpose, it is a major issue in the study-site to investigate the potential of big volume failures as well as the size of the blocks formed by the intersection of discontinuities on the cliff that will contribute to the formation of the blocks that are probable to reach the protection barriers.

Fig. 3 General view of the Solà d'Andorra above Santa Coloma (up) and close view of the Forat Negre rockfall sources and chute (down)

To obtain accurate topographical data, field work was performed which consisted in capturing topographical data using a TLS. The used device was an Optech Intelligent Laser Ranging and Imaging System (OPTECH-ILRIS3D), composed by a transmitter/receiver of infrared laser pulses and a scanning device. The average scanning distance from the slope was less than 600 m. Using a TLS the topographical relief is represented by a point cloud based on the distance and orientation of the points from the device, including the 3D coordinates of each point. Points were obtained every less than 1 cm approximately. More technical specifications on the use of TLS and the data acquisition can be found at Abellán et al. (2006 and 2009).

For the slope face of Forat Negre, a series of scans from two different stations was carried out to avoid missing points which are not visible from a given station. For one station two scans were needed to cover the entire zone of interest. Afterwards, the 3 point clouds were superimposed and aligned using the software POLYWORKS (InnovMetric©) to obtain a final 3D point cloud (Oppikofer et al., 2009).

During the laser scanning, objects wholly or partially hidden from the point of view of the scanner were not captured at the Lidar dataset, resulting in uncertainty about their presence or position in the scene. Moreover, as vegetation and trees are present in the area, after the removal of the respective points from the point cloud, the resolution of the DEM was locally affected. Thus a DEM of standard resolution had to be used for this application.

Based on the point cloud a moderate-precision 5 m contour DEM was also produced in ASCI format, with cell size 1x1 m^2.

3.2 Identification of discontinuity sets and failure mechanisms

The point cloud of the study-area, as represented by COLTOP3D is shown in Figure 4. The characteristics of every discontinuity set were assessed by calculating the average values of the dip and dip direction for selected representative subsets.

For each set, small representative groups of points were manually selected. For simplification their average dip and dip direction were assumed to be representative for the whole set, with a tolerance to consider their variation. For the study-area, 6 discontinuity sets were identified (Figure 5). Dip and dip direction for each set are selected so as the points that do not belong to the set (noise) to be excluded and the points that apparently belong to it to be included. Validation is made on visual inspection of the point cloud and photos of the study site. The tolerance value is different for each set. Comparison of the discontinuity sets with those found by field survey (Copons, 2004), show good convergence of the results. The most frequent are

J1 and J2. J3 often co-exists with J2, but due to the significant variation of their dip and dip direction they are considered separately. J4 and J5 alternate in the formation of unstable volumes intersecting the rest of the sets. J6 is very scarce over the slope and accordingly the corresponding volumes are few and they are not taken into account. The most important discontinuity sets J1 to J5 are present along the entire slope.

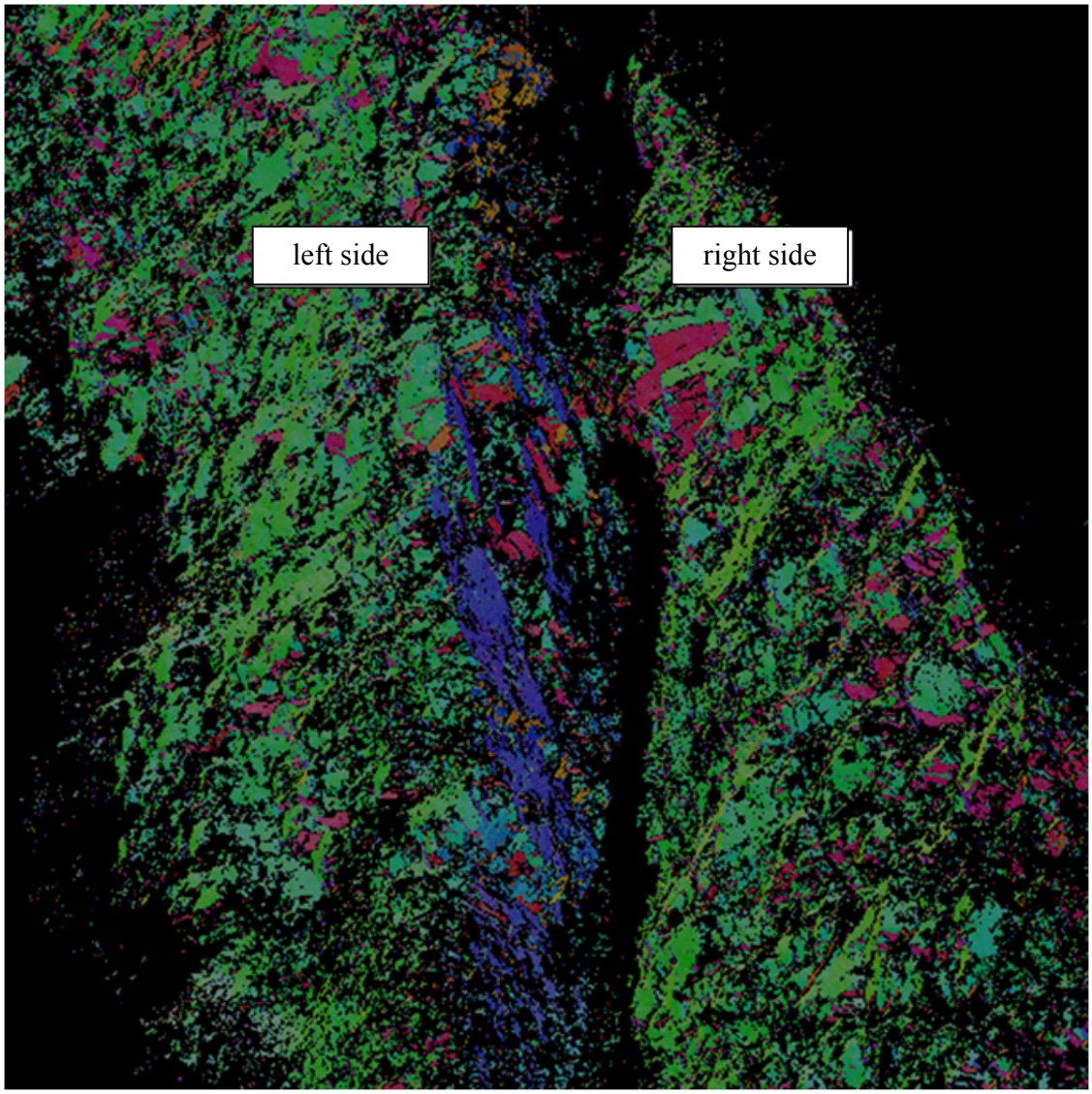

Fig. 4 Image of the point cloud in COLTOP3D. The 6 principal discontinuity sets are depicted with different colours (violet, fuchsia, orange, green, light blue, yellow).

Set	Colour	Dip Dir.	Dip	Tolerance
J1	Violet	56	65	20
J2	Fuchsia	322	72	15
J3	Orange	279	56	20
J4	Green	184	57	15
J5	Light blue	141	62	15
J6	Yellow	230	61	15

Fig. 5 Stereogram and principal discontinuities sets for the study site

Site inspection shows that plane failure is the predominant mechanism in the study site. Assuming sliding as the principal mechanism in generating rockfalls, the discontinuity sets J4 and J5 act unfavourably by comparison to the slope angle, permitting the detachment of rock volumes. J4 and J5 sets do not intersect each other; instead they alternate at the formation of the rock volumes.

3.3 Potentially unstable rock masses size distribution, PRSD

As indicated by the analysis of the discontinuity sets at the previous section, J4 and J5 are unfavourable discontinuity sets that permit the detachment of rockfalls. The slope orientation and angle of the topographic surface are compared with the dip direction and dip of these two sets, at every cell of a 1x1 m^2 resolution DEM, to produce the raster indicating in which cells failure is kinematically possible. Unions of adjacent cells producing large surfaces were also observed.

Using ArcMap tools, the obtained surfaces were superimposed on the orthophotos and marked with polygons. Additionally, after the observation of the orthophotos, smaller surfaces that stick out from the topographical relief and that correspond to separate smaller potentially unstable surfaces were detected inside the perimeter of those polygons. The application of the proposed procedure to Forat Negre is shown in Figure 6, where the polygons indicate the surfaces where both sets J4 and J5 are unfavourable. Given the vicinity of J4 and J5 at the stereogram, the surfaces on the projected DEM where these two sets are present, are common in their majority. 47 surfaces were detected in total, of which 9 on the left side and 38 on the right (Table 1).

The areas of these polygons were calculated as illustrated at the area-frequency diagram of Figure 7. They vary from 2 m^2 up to 1361 m^2 the biggest one. As afore-mentioned, big surfaces might correspond to the

union of smaller neighbouring surfaces on the two-dimensional DEM. This means that a rockfall with an area of 1361 m^2 is possible to be released from the slope face as a unique mass or, alternatively, through small successive failures. The areas of smaller surfaces inside the big ones were as well added separately into the dataset to build the area-frequency diagram, as it is not known a priori whether smaller or larger failures will take place.

The volume distributions were calculated for cubic and prismatic volumes from Equations (3) and (4). The cumulative diagrams are shown in Figure 8. The maximum kinematically removable rock masses that were indicated using this procedure are of the order of 50000 m^3 and 25000 m^3, for cubic and prismatic volumes respectively. This order of magnitude complies with the thresholds established for fragmental rockfalls (see Section 1). They represent big volumes which have never been previously observed in the study-site, but are kinematically possible. Table 1 shows the results of this analysis differentiating between the left and the right side of the chute. The most and largest instabilities were detected on the right side as also depicted in Figure 6, due to the slope's orientation.

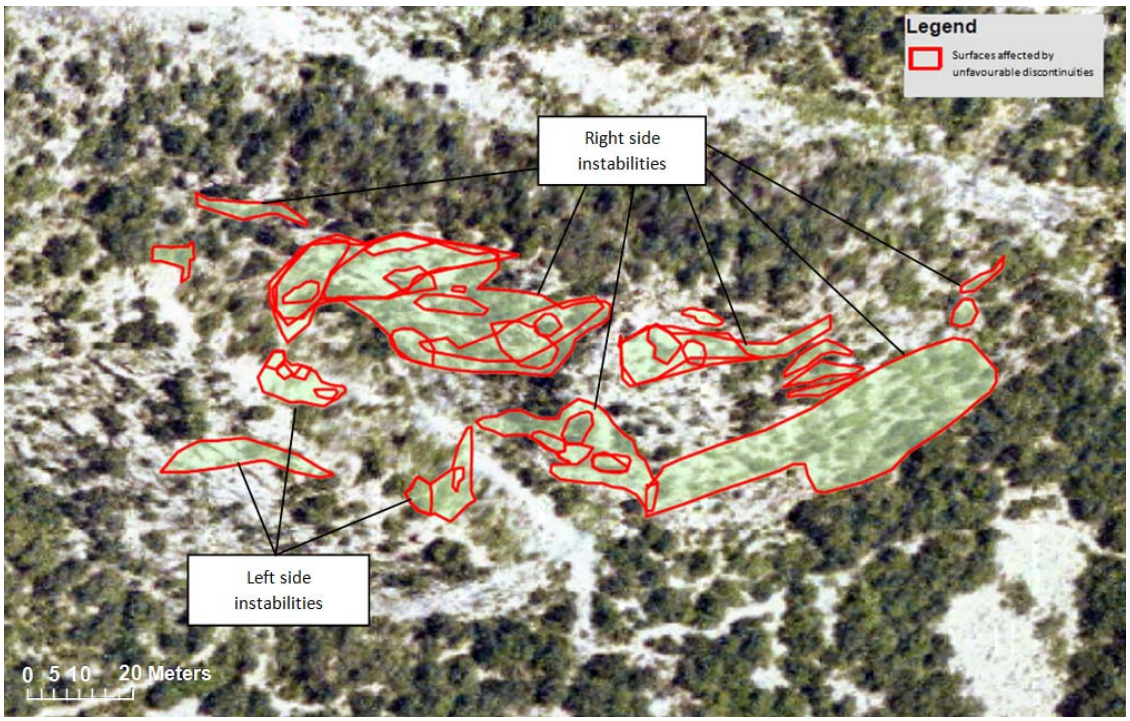

Fig. 6 The surfaces where the discontinuity sets J4 and J5 are unfavourable permitting the detachment of rockfall mass from the cliff face.

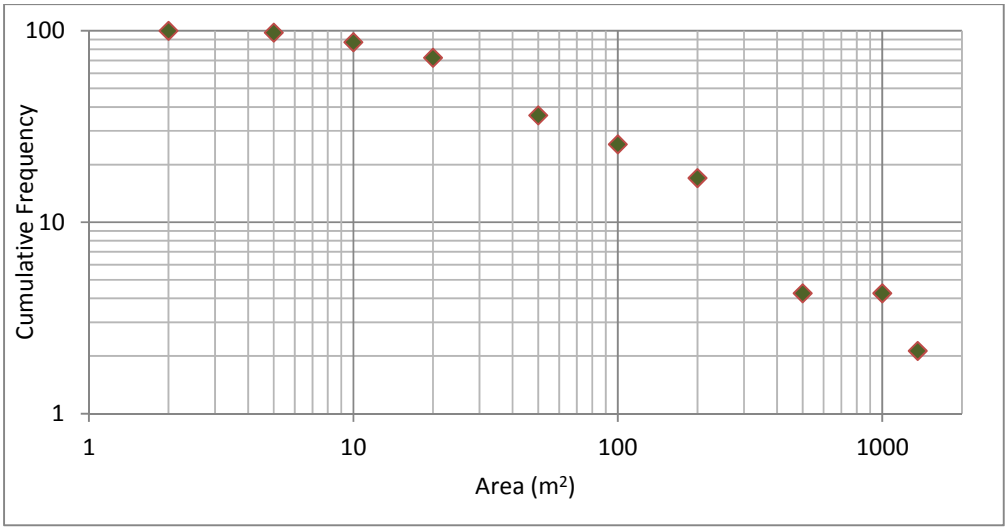

Fig. 7 Size distribution (cumulative frequency) of basal areas of potentially unstable rock masses

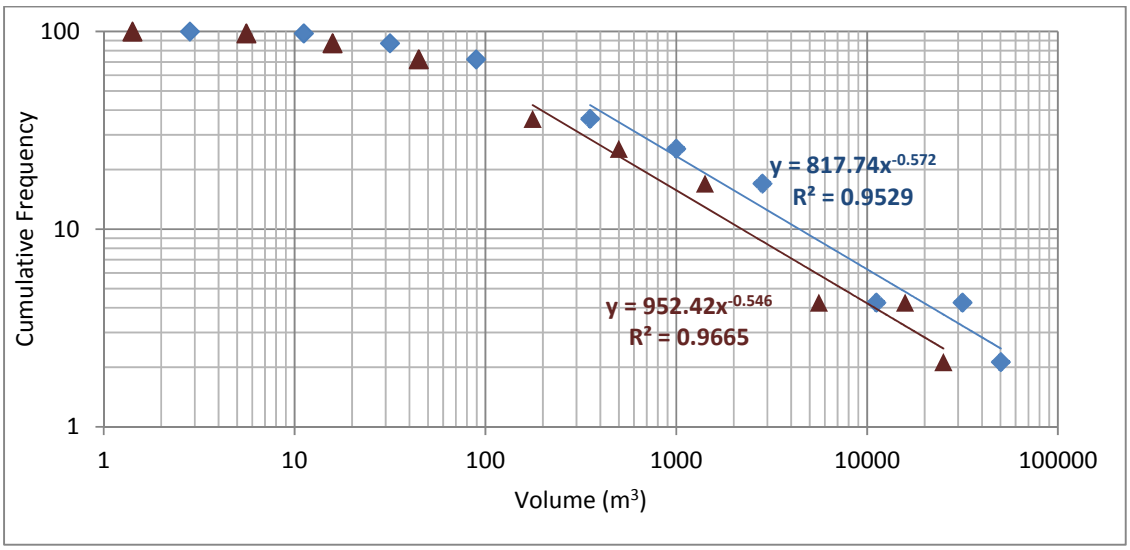

Fig. 8 PRSD –Potentially unstable rock masses size distribution for cubic (rhombus) and prismatic (triangles) shape . Power-law fitting for volumes corresponding to volumes equal or greater than 100 m^3.

Table 1. Size distribution (cumulative frequency) for the left and right side of the chute

Area (m2)	Volume - cube (m3)	Volume - prismatic (m3)	Cum. frequency - left side	Cum. frequency - right side
0-2	0-3	0-1	9	38
2-5	3-11	1-6	9	37

5-10	11-32	6-16	9	32
10-20	32-89	16-45	5	29
20-50	89-354	45-177	5	12
50-100	354-1000	177-500	5	7
100-200	1000-2828	500-1414	5	3
200-500	2828-11180	1414-5590	1	1
500-1000	11180-31623	5590-15811	0	2
1000-1361	31623-50210	15811-25105	0	1

As aforementioned correlating the rockfall size distribution with the frequency-magnitude relation was out of the scope of this paper. However, to check the results, the volume distribution of Figure 8 was compared against the volume of real events in the study-site and their relative frequency. The observed events of 25 m^3 are approximately two times more frequent than those of 150 m^3 (Corominas and Mavrouli, 2013). Using the data of Figure 8 for cubic and prismatic volumes, these ratios are 1.5 and 1.2 respectively. This means that in reality big volumes are less frequent than smaller ones in comparison with the calculated statistical ratio.

At the diagrams shown in Figure 7 and Figure 8, the frequency of small volumes (i.e. smaller than 50 m^3) is underestimated as the visual observation of the orthophotos does not permit the detection of all volumes sticking out from the topographical relief, or because rock masses of big areas and volumes do not necessarily fail as a single event. So to assess the power-law exponent for big rockfalls volumes, we considered volumes greater than 100 m^3. It was observed that big volumes follow a power-law with an approximate exponent of -0.5. This exponent is different than the one indicated by Santana et al. (2012) for the same study-site, where it was found that volumes corresponding to rockfall scars are well fitted by a power-law with an exponent of -0.9 approximately. The value of -0.9 yields smaller volumes that mostly approximate the observed small and intermediate events, without taking into account a potential stepped-path failure. Instead the exponent -0.5 corresponds to bigger volumes and has been assessed taking stepped-path failures into consideration.

3.4 In-situ rock block size distribution, IBSD

The second procedure also requires the discontinuity sets that were previously identified for the calculation of the PRSD. At first point, we defined the way that the discontinuities intersect each other on the cliff and contribute to the formation of the in-situ blocks. An example is shown in Figure 9. Close observation of the point cloud indicates that the potentially unstable rockfall volumes are formed by the intersection of the three following combinations of discontinuity sets (Figure 10):

- Volumes V1: J1+J2+J4

- Volumes V2: J1+J2+J5
- Volumes V3: J1+J3+J5

J4 and J5 form the sliding basal surface of the block. The volumes of type V1 and V2 are the most frequent. Volumes V1 are mainly present on the right side of the chute while volumes V2 on both sides. The volumes V3 are very scarce in the study site.

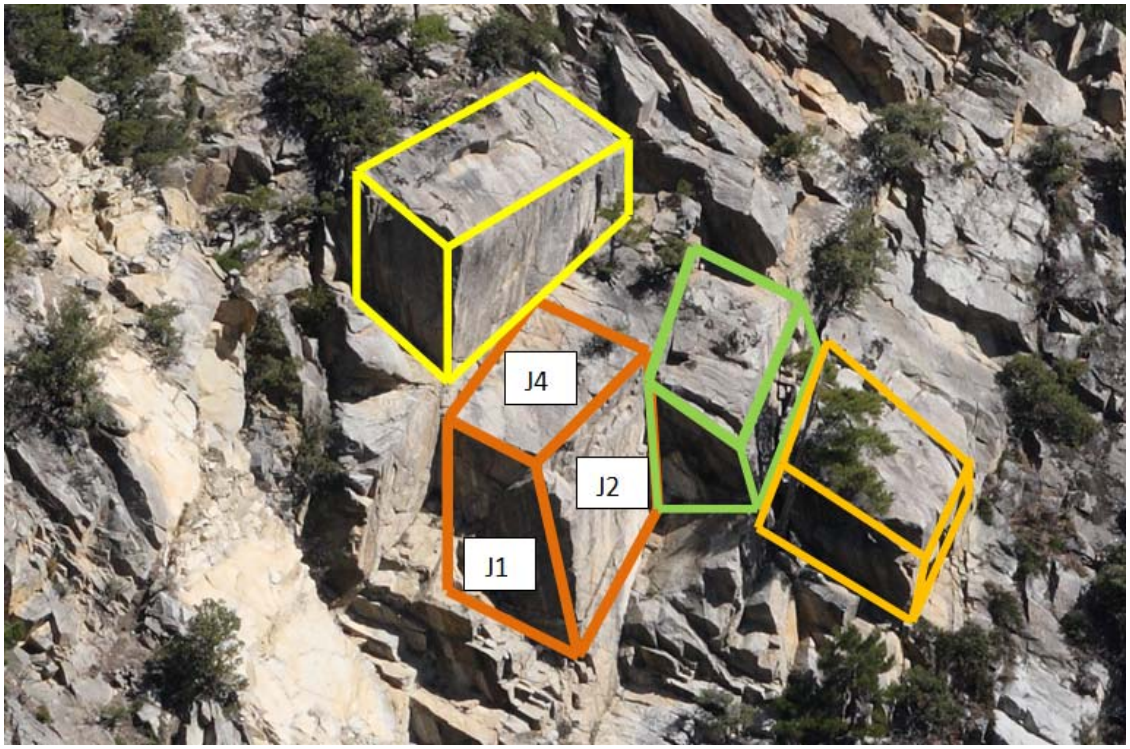

Fig. 9 Example of in-situ rock blocks in the study site (J1, J2 and J4 are discontinuity sets **)**

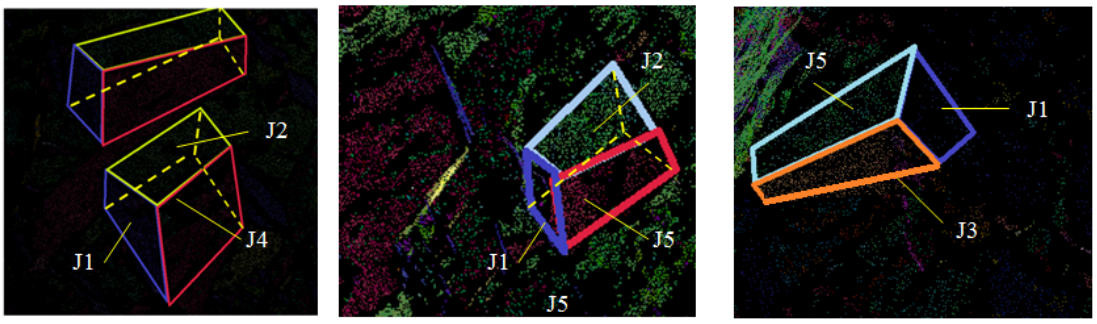

(a) (b) (c)

Fig. 10 Intersection of different discontinuity sets for the formation of unstable volumes: (a) volumes V1, (b) volumes V2, (c) volumes V3

The points of the TLS point cloud were grouped into discontinuity sets and exported to Polyworks. 6 groups of points were created, as many as the discontinuity sets. Then, separately for every group we detected visually the points corresponding to the exposed surfaces on the cliff and we fitted automatically a plane to each exposed surface (segment). The automatic fitting of a plane to the points belonging to the same segment was made by regression: once the current segment reached a predefined number of points (6) an orthogonal regression plane was fitted to it. To filter out points not belonging to the segment, the normal vector of a given candidate point was checked with reference to the normal vectors of all points included in a sphere with centre the candidate point and 1 m diameter. Candidate points with a normal vector deviating more than 45º with reference to their neighbouring points were filtered out. This angle was chosen to permit a certain undulation or rugosity of the surfaces. Figure 11 shows indicatively the fitted planes for the discontinuity set J1 at Polyworks.

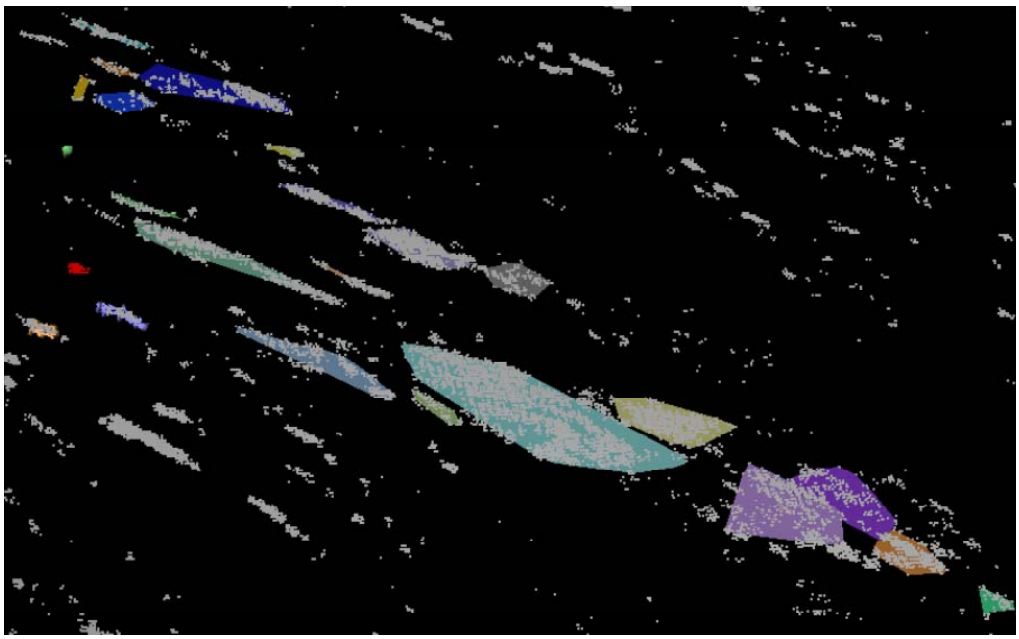

Fig. 11 Fitting of planes for the points cloud of the discontinuity set J1

The planes were then exported as polygons from Polyworks to Autocad v.10; the trace of all planes on an approximately perpendicular surface to them in the direction of their dip, were drawn separately for each set (one perpendicular surface was visually approximated here for all planes in the same set). Once the traces of the planes were defined, a representative window was selected for the characterisation of each set.

Sampling windows (Priest and Hudson 1981) were used to this purpose. The sample windows were selected to be representative of the density of joints compared with those observed in-situ. The selection of big sampling windows may incorporate errors related to not detected planes, thus small but representative ones are preferred. An indicative sample window for the discontinuity set J3 is shown in Figure 12.

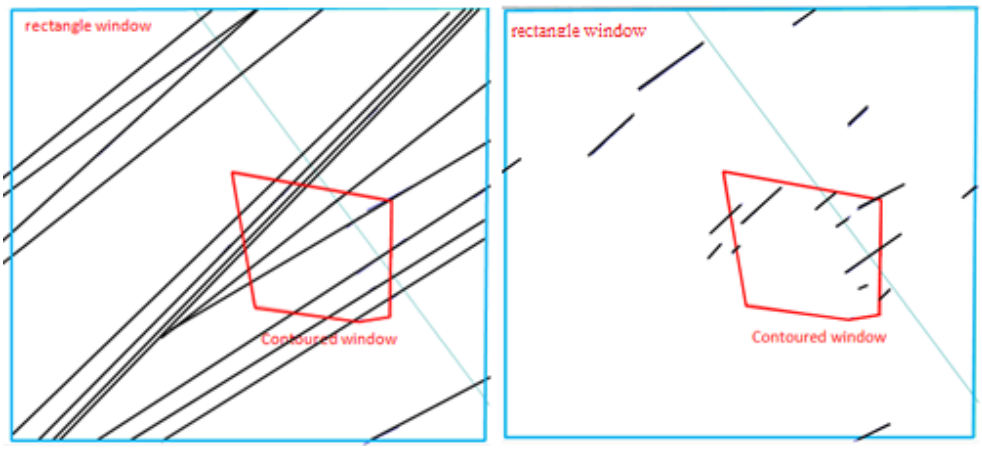

Fig. 12 Window sampling for the calculation of spacing for the discontinuity J3 considering joint of infinite persistence joints (case a –left) and (b) joints of finite persistence (case b – right)

The results for the average spacing, for infinite and finite persistence of the discontinuities are summarized at Table 2. In most cases, the results indicate approximately half spacing when fully persistent joints are considered rather than discontinuous. The discontinuities J2 and J4 for the case of finite persistence have higher values in comparison with the rest.

Table 2 Average spacing of discontinuity sets from the sampling window

Discontinuity set	Spacing assuming discontinuities of infinite persistence (theoretical case)	Spacing assuming discontinuities of finite persistence
	(m)	(m)
J1	1.6	3.7
J2	4.9	11.5
J3	0.7	1.6
J4	2.4	9.8
J5	1.2	3.6

Table 3 Average in-situ rock block volumes (m^3)

Intersecting discontinuity sets	Volumes for discontinuities of infinite persistence	Volumes for discontinuities of finite persistence
V1: J1+J2+J4	18	422
V2: J1+J2+J5	9	162
V3: J1+J3+J5	1	20

As the prisms angles are lower than 60°, according to Palmstrom (2005) Equation (6) can be directly applied using the average spacings of Table 2 as explained in section 2.4 and assuming that they follow the negative exponential distribution of Equation (5). Table 3 shows the average in-situ rock block volumes calculated by a Monte Carlo simulation, for 1000 samples for all the three discontinuity intersections (volume types V1 to V3), for the minimum theoretical spacings for joints of infinite persistence and of finite persistence. The standard deviation was also calculated to be 44, 40 and 3 m^3 for V1, V2 and V3 and discontinuities of infinite persistence and 1135, 436 and 56 m^3 for discontinuities of finite persistence respectively. Such values of the standard deviation indicate high spread of the data. The values of Table 3 also indicate the most expected sizes of the rock blocks for the study site on the theoretical condition that fractures take place exclusively along the pre-existent discontinuities and no new fractures are created. The volume of 422 m^3 is not a representative value for the studied chute as no fragments of that size have been registered so far in the study-site. This indicates that the values of spacings for discontinuities of finite persistence provide overestimated volumes, which is conservative.

Figure 13, based on the same Monte Carlo simulation, yields the IBSD for every intersection of discontinuities, for infinite or finite persistence assumptions. It is emphasised that the spatial distribution of all intersections of volumes cannot be calculated as the sum of the curves of Figure 13.

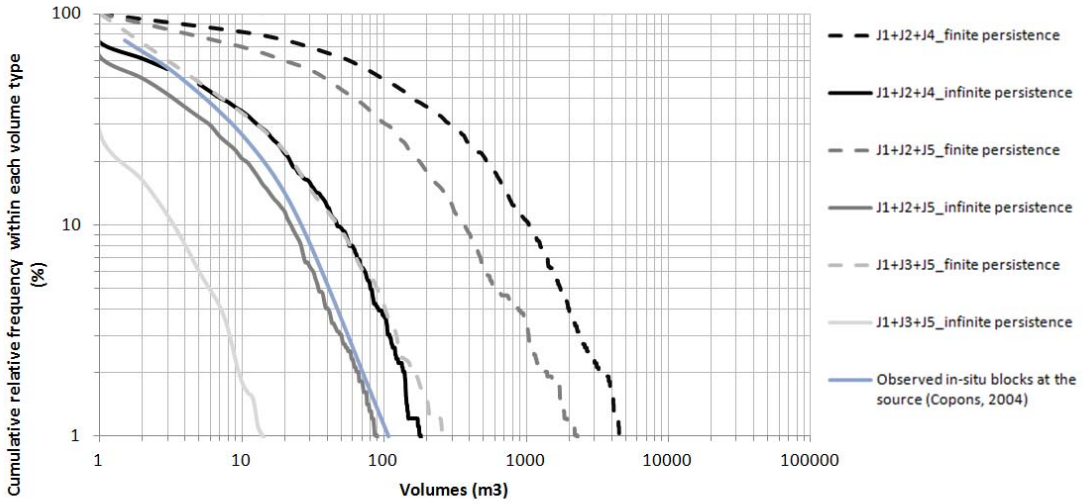

Fig. 13 IBSD for the average spacing of three intersections of discontinuities considering discontinuities of finite and of infinite persistence (volumes V1: J1+J2+J4, V2: J1+J2+J5, V3: J1+J3+J5) and the observed IBSD (Copons, 2004)

The maximum calculated values of the in-situ volumes are of the order of some thousands of cubic meters. The biggest volumes are defined by the combination of the J1, J2, J4 joint sets (volumes V1) considering finite persistence, thus the presence of rock bridges. For V1, 10% is greater than 1000m^3. Volumes V2 (J1+J2+J5) and of finite persistence may also give blocks of the same order of magnitude (4.5% of the volumes are greater than 1000 m^3). Volumes V3 for finite persistence, as well as V1 for infinite persistence give rock blocks of the order of some hundreds of cubic meters (3% exceeds 100 m^3) while V2 and V3 for infinite persistence are of some decades of cubic meters. For the study-site and especially for the chute of Forat Negre, the largest registered block reaching the foot of the rockfall cone has been 46 m^3, which is of the order of magnitude of the in-situ block volumes calculated for discontinuities of infinite persistence.

4 Discussion

In Forat Negre, the maximum in-situ observed block volume at the source area (on the rocky slope) is 184 m^3 and at the wider area is 270 m^3 (Copons, 2004). The calculated volumes which are greater than 184 m^3 correspond to percentages lower than 50% (approximately 40% for V1, 25% for V2 and 1.5% for V3, for finite discontinuities and less than 2% for V1 for infinite discontinuities).

For the two assumed persistences and for 1% cumulative relative frequency there is a difference of one or two orders of magnitude in the volumes: for V1 it is reduced from 4500 m^3 to 200 m^3 (23 times smaller for infinite persistence), for V2 from 2100 m^3 to 90 m^3 (23 times smaller) and for V3 from 250 m^3 to 15 m^3

approximately (17 times smaller). This shows the importance of the persistence and the formation of rock bridges in the rock mass for the size distribution of rock blocks.

To check the consistency of these results with real observations, we plotted a curve with the field data for the observed in-situ blocks measured by Copons (2004) in the source area, as seen in Figures 13 and 14. Those volumes have been defined on the slope face by volumetric analysis of the blocks bounded by the existing discontinuity sets, by direct measurement of the nearly detached blocks, and by estimation of their size from photos. The plotted curve is better approximated by the case of discontinuities of infinite persistence (Figure 14). This leads to the conclusion that for the study-site which is intensely fractured, evaluating the persistence only by the visible trace length of the discontinuities is a very conservative assumption. Instead the size distribution of the in-situ blocks is better approximated in the theoretical case of infinite discontinuities, although in some cases this may lead to underestimation of big volumes. It can be deducted that discontinuities have a finite persistence which is high and close to the theoretical case of infinite persistence, although not the same.

Power-law distributions were fitted to the data, which were all found to have an exponent of -1.3 approximately, with the exception of the volumes V3 for infinite discontinuities, which are fitted by a power law with an exponent -1.70. Field data also were well fitted by a power-law distribution with an exponent of -1.4 for volumes higher than 11 m^3 (for smaller volumes the fitting was not satisfactory), which is a good approximation of the results. Fig. 14 indicates that the power-laws, despite their high r^2 coefficient, fit the right part of the curves but for the left part they fail to describe satisfactorily the relative frequency. The similarity of these exponents indicates that at least some parts of these curves have similar shape. This is an evidence of repetition at the rock block patterns, possibly related to the process of the structural formation of the slope.

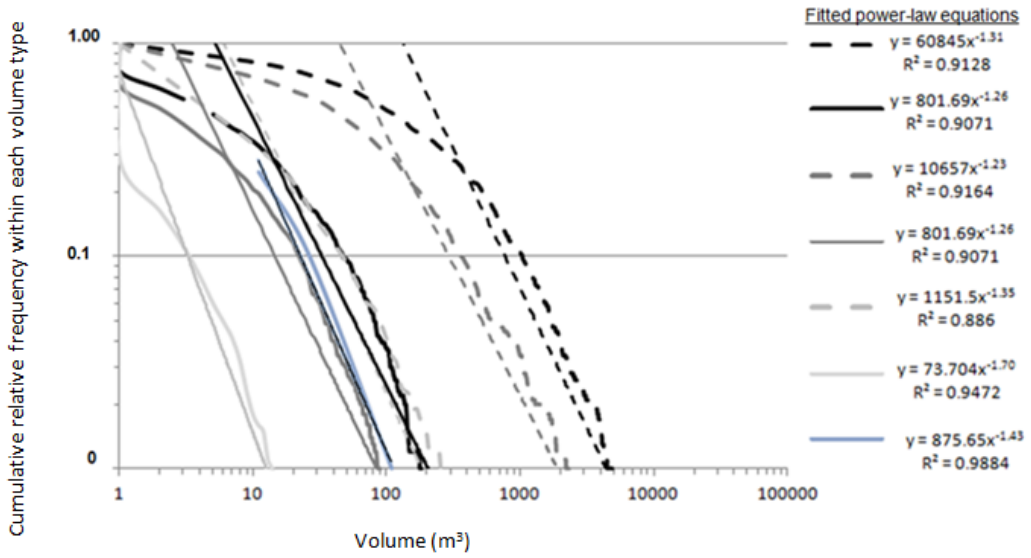

Fig. 14 Power-law fitting of the calculated IBSD (volumes V1: J1+J2+J4, V2: J1+J2+J5, V3: J1+J3+J5) and of the observed IBSD (Copons, 2004)

The probabilistic calculation of the rock block volumes was based on the assumption of a negative exponential distribution, however it still remains to investigate whether there is a physical limit of spacing that would imply the truncation of the exponential distribution, and thus impeding the formation of blocks above a certain size.

In some cases, during the impact with the ground there is the possibility of segmentation of the detached rockfall mass not only along the pre-existing planes of the discontinuity sets but also by propagation and coalescence of the discontinuities into the rock bridges or by the development of new cracks in the intact part of the rock. The blocks deposited downslope in the study area might be the result of all these segmentation processes. As the segmentation along rock bridges or new cracks has not been investigated for the study area, the IBSD cannot be compared with the curve of blocks deposited downslope, also measured by Copons (2004).

5. Conclusions

In this paper an alternative methodology was presented for:

(1) The calculation of the potentially unstable rock masses size distribution PRSD that refers to big volumes corresponding to rare events with low susceptibility of failure, by detection of kinematically unstable surfaces on a DEM and on orthophotos.

(2) The assessment of the in-situ rock blocks size IBSD distribution on the slope face, by calculation of the equivalent volume of the prisms which are formed by the intersection of the existing discontinuity sets.

A high-resolution DEM is needed, especially for (2). Both procedures are independent from the existence of past data and may be used to overcome limitations related to access restrictions and high field work costs. Further advantages of the procedures are that they are simple, they need few input data and they can provide results at massive scale.

The obtained information can provide some clues for the rockfall magnitude frequency relation and the size distribution of the fallen blocks during the process of rockfall hazard and risk assessment, especially when it comes to their quantification; however this has not been investigated here.

The first proposed procedure is based on assumptions describing a conservative scenario of very low probability, such as that (a) the potential rockfall mass is detached entirely at a single rockfall event, without taking into account that smaller successive failures are possible instead, (b) all discontinuity sets are present everywhere in the slope - the important joint sets are spread all over the slope as observed on

the DEM- and they have infinite persistence and (c) big stepped-path failures are possible. The presence and intersection of persistent joints that kinematically permit the detachment of rocks from the slope face in every cell of the DEM in reality has a very low probability. This is why these volumes correspond to rare events with low susceptibility of failure and their distribution may differ from the one for the usually observed volumes.

Larger rock mass volumes than those calculated with this procedure might be possible for slopes with one predominant and continuous discontinuity set and with scarcity of discontinuities intersecting it, but this case is not discussed here. This procedure is not recommendable for the size distribution of volumes smaller than 100 m^3 because these volumes might be underestimated as they are not easily detectable by visual observation of the orthophotos.

Its application to Forat Negre indicated potentially unstable rock masses of the order of 50000 m^3 and 15000 m^3, for cubic and prismatic volumes respectively, but as explained with low susceptibility to failure. The fitting of the calculated data for cubic and prismatic volumes greater than 100 m^3 by a power-law, indicated an approximate exponent of -0.5. This exponent is smaller than the one assessed by Santana et al. (2012) for rockfall scars, as it additionally considers the possibility of stepped-path failures. This value is suggested to be used for the size distribution of big rockfall volumes in the study-site although the volume may be overestimated because only one failure event is considered for each basal discontinuity surface.

It is necessary to emphasise that this work provides information on the potential unstable volumes on rocky slopes. However for the evaluation of the instability it is necessary to perform further investigation (for example using limit-equilibrium analysis) and also taking into account the cohesion and friction -based resistances and the effect of triggering factors.

Using the second procedure, it is possible to calculate the size distribution of the in-situ rock blocks using point cloud data from a Terrestrial Laser Scanner. To minimise errors due to shadowing or occlusion a DEM obtained by photogrammetry can be used to complement TLS data.

The results are very sensitive to the selection of a representative area that is used as the sample window for the spacing measurements. Visual validation of the area of the sample window and of its representativity for the entire slope is suggested, if possible.

The effect of persistence is different for the PRSD (section 2.3) and the IBSD (section 2.4). When referring to the PRSD for which the stability or instability are checked at every cell of the DEM, when two or more cells are found to be unstable they are summed up to give the total unstable mass. This practically means that big unstable rock masses involve two or more joints of the same set but at different levels in their interior. Thus the higher the persistence, the higher the presence of joints along the slope and the bigger are the volumes that might be formed. Instead for IBSD the effect of the persistence is different. As the rock blocks are defined by just two successive joints of the same set, no joints are included in the interior of the rock blocks and joints of higher persistence present more frequent intersections and define smaller blocks.

The application of the second procedure to the study-site indicated a correlation between the persistence of the joints and the maximum formed in-situ rock block volumes. The difference between the spacings of the expected equivalent prismatic volumes for the two extreme cases of infinite discontinuities (theoretical case) and finite discontinuities (considering only the visible trace length at each plan) is of one order of magnitude. Comparison of the calculated size distributions for the three volume types V1 to V3 (formed by the three discontinuity intersections) with the observed data showed that for the study-site which is intensely fractured, evaluating the persistence only by the discontinuities visible trace length at each plane is an assumption that provides overestimated volumes, thus is conservative. Instead, the in-situ block distribution, IBSD, which was observed on the slope face, is better fitted by the calculated in-situ block distributions for the theoretical case of infinite persistence of the discontinuities. This observation indicates that in the study area the discontinuities have a very high persistence.

The size distribution of the in-situ rock blocks IBSD at the source for the considered discontinuity intersection and persistence assumptions can be well fitted by a power-law relation with an exponent -1.3, when the respective exponent for the observed volumes is very close to this value and equal to -1.4. This indicates that the rock block size distribution presents a certain statistical character which is related to the network of the discontinuity sets in the slope, as resulting from the process of its structural formation. The exponent -0.9 found by Santana et al. (2012) for the rockfall scars at the study-site indicated that the latter in most cases are composed by various in situ-blocks.

Acknowledgements

This work has been supported by the Marie Curie Research and Training Network "Mountain Risks" funded by the European Commission (2007–2010, Contract MCRTN- 35098) and by the Government of Andorra (Edicte de 10/04/2013, BOPA nº18 17/04/2014). The authors would like to thank A. Loye, A. Pedrazzini and C. Longchamp for their support in the preparation of this work.

References

Abellán A, Vilaplana JN, Martínez J (2006) Application of a long-range Terrestrial Laser Scanner to a detailed rockfall study at Vall de Núria (Eastern Pyenees, Spain). Engineering Geology 88: 136-148

Abellán A, Jaboyedoff M, Oppikofer T, Vilaplana JM (2009) Detection of millimetric deformation using a terrestrial laser scanner: experiment and application to a rockfall event. Nat. Hazards Earth Syst. Sci. 9: 365–372

Aler J, Du Mouza J, Arnould M (1996) Measurement of the Fragmentation Efficiency of Rock Mass Blasting and its Mining Applications. Int. J. Rock Mech. Min. Sci. Geomech. 33(2): 125-139

Barton N (2013) Shear strength criteria for rock, rock joints, rock fill and rock masses: Problems and some solutions. Jour. of Rock Mech.and Geotech. Eng. JRMGE Wuhan Elsevier 5: 249-261

Becker J, Stewart C, Radke RJ (2009) LiDAR inpainting from a single image. IEEE 12th International Conference on Computer Vision. Proceedings of International Conference on 3-D Digital Imaging and Modeling (3DIM).

Birch J S (2006) Using 3DM Analyst mine mapping suite for rock face characterization. In Laser and Photogrammetric Methods for Rock Face Characterization ARMA (Ed) Tonon F, Kottenstette J. 13–32

Chau KT, Wong RHC, Wu JJ (2002) Coefficient of restitution and rotational motions of rockfall impacts. Int J Rock Mech Min Sci. 39:69–77

Coggan J S, Wetherelt A, Gwynn XP, Flynn ZN (2007) Comparison of hand-mapping with remote data capture systems for effective rock mass characterization. Proceedings of the 11th Congress of ISRM, July 2007, Lisbon, Portugal.

Copons R (2004) Avaluació de la perillositat de caigudes de blocs a Andorra la Vella (Principat d'Andorra) Ph.D. thesis. UB Barcelona

Corominas J, Mavrouli O (2013) Estimation quantitative du risque (QRA) pour les bâtiments lié aux éboulements rocheux progrès et défis. Les dangers naturels en Suisse: pratique et développements. In Comptes rendus de la deuxième Journée de Rencontre sur les Dangers Naturels (Université de Lausanne, 18 février 2011). Mémoire de la Société vaudoise des Sciences naturelles. (Ed) Nicolet P., Derron M-H and Jaboyedoff M. 25 : 229-242.

Corominas J, Mavrouli O, Moya J (2012) Simplified approach for obtaining the block volume distribution of fragmental rockfalls. ISL-NASL 2012. 11th International & 2nd North American Symposium on Landslides. 3-8 June Banff: CRC Press. Taylor & Francies Group. 1159-1164

Crosta G, Agliardi F (2003) A methodology for physically based rockfall hazard assessment. Natural Hazard and Earth Systems Science. 3:407–422

Cruden DM, Hungr O (1986) The debris of the Frank Slide and theories of rockslide–avalanche mobility. Canadian Journal of Earth Sciences. 23(3): 425-432

Cruden DM, Varnes DJ (1996) Landslide types and processes. In Landslides: Investigation and Mitigation. (Ed)Turner AK, Shuster R.L. Transp Res Board. Spec Rep 247: 36–75

Délèze JY, Jaboyedoff M, Baillifard F, Rouiller JD (2003) Mattercliff - software for the analysis of spatial distribution of discontinuities in cliffs. EGS - AGU - EUG Joint Assembly, Nice, France, April 2003. Geophysical Research Abstracts, vol. 5, 03384

Derron MH, Blikra L, Jaboyedoff M (2005) Preliminary Assessment of Landslide and Rockfall Hazards using a DEM (Oppstadhornet, Norway). Natural Hazards and Earth System Sciences. 285–292

Di Luzio E, Bianchi Fasani G, Bretscheider A (2013) Potential rockfalls and analysis of slope dynamics in the Palatine Aarchaeological area (Rome, Italy) Geologica Acta , Vol . 11 , N º 2 , June 2013 , 245 – 264.

Dorren LKA, Domaas U, Kronholm K, Labiouse V (2011) Methods for predicting rockfall trajectories and run-out zones. In: S. Lambert & F. Nicot (eds.). Rockfall engineering. ISTE Ltd. / John Wiley & Sons Inc. 143 - 173

Dussauge-Peisser A, Helmstetter C, Grasso JR, Hantz D, Desvarreux P, Jeannin M, Giraud A (2002) Probabilistic approach to rockfall hazard assessment: potential of historical data analysis. Natural Hazards and Earth Systems Sciences 2: 15-26

Elmouttie M, Poropat G (2011) A method to estimate in situ block size distribution. Rock Mech Rock Eng. 37:529–535

Evans SG, Clague JJ, Woodsworth, G J (1989) The pandemonium Creek Rock Avalanche, British Columbia. Canadian Geotechnical Journal. 26 (3): 427-446

Evans S, Hungr O (1993) The assessment of rockfall hazard at the base of talus slopes. Can. Geotech. J. 30: 620–636

Gates W, Ortiz L, Florez R (2005) Analysis of Rockfall and Blasting Backbreak Problems, US 550, Molas Pass, CO. 40th U.S. Symposium on Rock Mechanics (USRMS), June 25 - 29, Anchorage, Alaska

Gaich A, Poetsch M, Schubert W (2006) Acquisition and assessment of geometric rock mass feature by true 3D images, in: Proceedings of the 41st U.S. Symposium on rock mechanics (USRNS). 17–21 June.Golden, Colorado

Grasselli G (2001) Shear Strength of Rock Joints Based on Quantified Surface Description, Ph.D. dissertation, Ecole Polytechnique Fédérale de Lausanne

Guerin A, Hantz D, Rossetti1 J- P, Jaboyedoff M. (2014) Estimating rockfall frequency in a mountain limestone cliff using terrestrial laser scanner Nat. Hazards Earth Syst. Sci. Discuss. 2: 123–135 (under review)

Guzzetti F, Reichenbach P, Wieczorek G F (2003) Rockfall hazard and risk assessment in the Yosemite Valley California, USA. Natural Hazards and Earth System Sciences. 3: 491-503

Hack HRGK (1998) Slope Stability Probability Classification, SSPC. ITC publications no 43. Delft.

Hantz D (2011) Quantitative assessment of diffuse rock fall hazard along a cliff foot. Nat Hazards Earth Syst Sci. 11: 1303–1309.

Hoek E, Bray J (1981) Rock slope engineering. The Institution of Mining and Metallurgy, London

Hsü KJ, Kenneth J (1975) Catastrophic Debris Streams (Sturzstroms) Generated by Rockfalls. Geological Society of America Bulletin 86 (1): 129–140

Hungr O, Evans SG, Hazzard J (1999) Magnitude and frequency of rock falls and rock slides along the main transportation corridors of southwestern British Columbia. Canadian Geotechnical Journal. 36 (2): 224-238

Hungr O, Leroueil S, Picarelli L (2014) The Varnes classification of landslide types, an update. Landslides. 11(2):167-194

Jaboyedoff M, Baillifard F, Hantz D, Heidenreich B, Mazzoccola D (2001) Terminologie. In Prévention des mouvements de versants et des instabilités de falaises. (Ed) Carere K, Ratto S, Zanolini FE. 48–57.

Jaboyedoff M, Baillifard F, Philippossian F, Rouiller JD (2004) Assessing fracture occurrence using "weighted fracturing density": a step towards estimating rock instability hazard. Natural Hazards and Earth System Sciences. 4: 83-93

Jaboyedoff M, Couture R, Locat P (2009) Structural analysis of Turtle Mountain (Alberta) using digital elevation model: toward a progressive failure. Geomorphology. 103: 5-16

Jaboyedoff M, Dudt JP, Labiouse V (2005) An attempt to refine rockfall hazard zoning based on the kinetic energy frequency and fragmentation degree. Natural Hazards and Earth System Sciences. 5: 621–632

Jaboyedoff M, Metzger R, Oppikofer T, Couture R, Derron MH, Locat J, Turmel D (2007) New insight techniques to analyze rock-slope relief using DEM and 3D-imaging cloud points: COLTOP-3D software. In Rock mechanics: Meeting Society's Challenges and demands (Vol. 1) Taylor & Francis (Ed) Eberhardt E, Stead D, Morrison T. 61-68.

Jaboyedoff M, Oppikofer T, Abellan A, Derron MH, Loye A, Metzger R, Pedrazzini A (2012) Use of LIDAR in landslide investigations: an overview. Natural Hazards. 61:5-28.

Jaboyedoff M, Philippossian F, Mamin M, Marro C, Rouiller JD (1996) Distribution spatiale des discontinuités dans une falaise. Rapport de travail PNR31, VDF Publisher, Zürich. pp 90

Kemeny J, Norton B, Turner K 2006. Rock slope stability analysis utilizing ground-based LiDAR and digital image processing. Felsbau.24: 8–16.

Kemeny J, Post R (2003) Estimating Three-Dimensional Rock Discontinuity Orientation from Digital Images of Fracture Traces. Computers and Geosciences. 29(1): 65-77

Kemeny J, Turner K (2008) Ground based LIDAR. Rock slope Mapping and assessment. Technical report of the Central Federal Lands. Highway Division US Department of Transportation FHWA-CFL/TD-08-006 (www.iaeg.info)

Kim BH, Cai M, Kaiser PK, Yang HS (2007) Estimation of Block sizes for rock masses with non-persistent joints. Rock Mechanics and Rock Engineering. 40(2): 169-192

Krishna C, Devkota J, Eun H, Gyo-Won K (2009) Characteristics of discontinuity spacing of Yeongdeok granite. Geosciences Journal. 13(2): 161-165

Kulatilake PHSW, Chen J, Teng J, Pan G, Shufang X (1995) Discontinuity network modelling of the rock mass around a tunnel close to the proposed permanent shiplock area of the three gorges dam site in China. Proceedings od 35th U S Rock Mechanics Symposium (Ed) Daemen and Schultz. 807–812

Lato M, Hutchinson J, Diederichs M, Ball D, Harrap R (2009) Engineering monitoring of rockfall hazards along transportation corridors: using mobile terrestrial LiDAR. Nat Hazards Earth Syst Sci. 9: 935–946 .

Lizotte YC, Scoble MJ (1994) Geological control over blast fragmentation. Canadian Mining and Metallurgical Bulletin. 87(983). 57-71 .

Locat P, Couture R, Locat J, Leroueil S, Jaboyedoff M (2006) Fragmentation energy in rock avalanches. Can J Geotech. 43: 830-851

Lu P, Latham JP (1999) Developments in the assessment of in-situ block size distributions for rock masses. . Rock Mech Rock Eng. 32:29-49

Markland J T (1972) A useful technique for estimating the stability of rock slopes when the rigid wedge slide type of failure is expected. Imperial College Rock Mechanics. Research Reprints. 19: pp 10

Metzger R, Jaboyedoff M, Oppikofer T, Viero A, Galgaro A (2009) Coltop3D: A New Software for Structural Analysis with High Resolution 3D Point Clouds and DEM. Frontiers + Innovation CSPG CSEG CWLS Convention. Calgary, Alberta (Canada) .

Moya J, Corominas J, Pérez Arcas J, Baeza C (2010) Tree-ring based assessment of rockfall frequency on talus slopes at Solà d'Andorra, Eastern Pyrenees. Geomorphology. 118: 393–408

Nocilla N, Evangelista A, Scotto di Santolo A (2009) Fragmentation during Rock Falls: Two Italian Case Studies of Hard and Soft Rocks. Rock Mech Rock Eng. 42:815–833. DOI 10.1007/s00603-008-0006-0

Oppikofer T (2009) Detection analysis and monitoring of slope movements by high-resolution digital elevation models. PhD thesis. Istitute of Geomatics and Analysis of Risks. Faculty of Geosciences and Environments. University of Lausanne. Switzerland

Oppikofer T, Jaboyedoff M, Blikra LH, Derron MH, Metzger R (2009) Characterization and monitoring of the Åknes rockslide using terrestrial laser scanning. Natural Hazards and Earth System Sciences. 9: 1003-1019

Palmstrom A (2005) Measurement of and correlations between block size and rock quality designation (RQD) Tunelling and Underground Space Technology. 20: 362-377

Poropat G V (2006) Remote 3D mapping of rock mass structure. In Laser and Photogrammetric Methods for Rock Face Characterization ARMA. (Ed) Tonon F, Kottenstette J. 63–75, 2006

Priest SD, Hudson JA (1981) Estimation of discontinuity spacing and trace length using scan line surveys. Int J Rock Mech Min Sci & Geomech Abstr. 18: 183–197

Rohmer J and Dewez T (2012) What if the power-law model did not apply for the prediction of very large rockfall events? Geophysical Research Abstracts
Vol 14 EGU2012-2397

Santana D, Corominas J, Mavrouli O, Garcia-Sellés D (2012) Magnitude–frequency relation for rockfall scars using a Terrestrial Laser Scanner. Engineering Geology. 145-146: 50-64

Scholtès L, Donzé F-V (2012) Modelling progressive failure in fractured rock masses using a 3D discrete element method. International Journal of Rock Mechanics & Mining Sciences. 52:18–30

Slob S, Hack R (2004) 3D terrestrial laser scanning as a new field measurement and monitoring techniques. Engineering geology for infrastructure planning in Europe: a European perspective . Lectures Notes in Earth Sciences. Springer. Berlin/Heidelberg. 104:179–189

Slob S, Hack R, van Knapen B, Kemeny J (2005) A method for automated discontinuity analysis of rock slopes with 3D laser scanning. Proceedings of the Transportation Research Board (TRB) 84th Annual Meeting. Washington D.C.

Sornette D (2002) Predictability of catastrophic events: Material rupture, earthquakes, turbulence, financial crashes and human birth. Proc Natl Acad Sci. U S A. 99(1): 2522–2529

Sturzenegger M, Stead D (2009) Quantifying discontinuity orientation and persistence on high mountain rock slopes and large landslides using terrestrial remote sensing techniques . Natural Hazard and Earth System Sciences. 9 (2): 267-287

Turner K, Kemeny J (2005) A method for automated discontinuity analysis of rock slopes with three - dimensional laser scanning . In: Transportation research record: journal of the transportation research board .1913: 187-194

Varnes DJ (1958) Landslide types and processes. In Landslides and Engineering Practice. Highway Research Board Special Report 29. Washington D C. NAS-NRC Publication 544 (Ed) Eckel EB . 20 - 47

Varnes DJ (1978) Slope movement types and processes. In: Schuster R. L. & Krizek R. J. Ed., Landslides, analysis and control. Transportation Research Board Sp. Rep. No. 176, Nat. Acad. oi Sciences: 11–33

Wallis PF, King MS (1981) Discontinuity spacings in a crystalline rock. Int J Rock Mech Min Sci. 17: 63–66

Wang Y, Tonon F (2010) Discrete element modeling of rock upon Impact in rock fall analysis. Rock Mech Rock Eng. 44(1): 23-35

Zhang ZX, Kou SQ, Jiang LG, Lindqvist PA (2000) Effects of loading rate on rock fracture: fracture characteristics and energy partitioning . Int J Rock Mech Min Sci. 37:745–62